Diffusion of Ge in $Si_{1-x}Ge_x$/Si single quantum wells in inert and oxidizing ambients

Michelle Griglione[a] and Timothy J. Anderson
Department of Chemical Engineering, University of Florida, Gainesville, Florida 32611

Yaser M. Haddara
Cypress Semiconductor Corporation, San Jose, California 95134

Mark E. Law
Department of Electrical and Computer Engineering, University of Florida, Gainesville, Florida 32611

Kevin S. Jones
Department of Materials Science and Engineering, University of Florida, Gainesville, Florida 32611

Alex van den Bogaard
Laboratory of ECTM, DIMES, Delft University of Technology, Delft, The Netherlands

(Received 4 November 1999; accepted for publication 1 May 2000)

The interdiffusion of Si/$Si_{0.85}Ge_{0.15}$/Si single quantum well (SQW) structures subjected to inert- and oxidizing-ambient annealing was investigated as a function of temperature (900–1200 °C) and time. Point defect injection allowed modification of the vacancy and interstitial mediated components of interdiffusion, D_V and D_I. Diffusion profiles of samples processed in inert and oxidizing ambients were similar, which indicates a vacancy-dominated mechanism. Activation energies of diffusion in inert and oxidizing ambients were found to be 5.8 and 5.0 eV, respectively. A fractional interstitial component f_I of ~0.10 was estimated for the lower temperatures, while a significantly smaller f_I of ~0.02 was estimated for the higher temperatures. Experiments using SQWs with buried boron marker layers showed that dislocations in the $Si_{1-x}Ge_x$ trap point defects and affect interdiffusion behavior. © *2000 American Institute of Physics.* [S0021-8979(00)05015-5]

INTRODUCTION

Considerable interest exists in alloys of silicon and germanium ($Si_{1-x}Ge_x$) for applications in electronics and photonics. Devices incorporating Si–Ge solid solutions show increased speeds as well as other desirable features over the equivalent elemental Si devices. The manufacture of these devices includes several high-temperature and oxidation steps, and it is necessary that $Si_{1-x}Ge_x$ heterostructures be able to withstand these processing steps without device degradation produced by interface broadening and intermixing of the device layer structure. Therefore, it is important to understand the diffusion processes that cause degradation.

An important application for $Si_{1-x}Ge_x$ material is heterojunction bipolar transistor technology,[1–3] which uses doped $Si_{1-x}Ge_x$ as the base and surrounding Si layers as the emitter and collector regions. Diffusion of both the Ge and dopant from the base during growth and processing can form parasitic barriers at the heterojunctions, which severely degrades device performance. It is therefore important to be able to predict the influence of parameters such as anneal time and temperature, alloy composition, and strain state on the interdiffusion behavior of these Si/$Si_{1-x}Ge_x$/Si single quantum well (SQW) structures.

In this study, interdiffusion of Si/$Si_{0.85}Ge_{0.15}$/Si SQW heterostructures in inert and oxidizing ambients over a temperature range 900–1200 °C has been investigated. The Ge diffusion coefficient and thermal activation energy have been extracted by comparing secondary ion mass spectrometry (SIMS) profiles of annealed samples with those predicted by the Florida Object Oriented Process Simulator (FLOOPS).[4,5] This is a computer simulation program which predicts the diffusion profile of a semiconductor material after processing steps, by numerically solving modified versions of Fick's law. It is generally accepted that thermal oxidation of the silicon surface injects excess interstitials into the bulk material.[6,7] The proportional dependence of a material's self-diffusion mechanism or dopant's diffusion mechanism on these defects can be determined by monitoring any enhancement or retardation of the diffusion with the addition of these defects. Thermal processing of Si/$Si_{0.85}Ge_{0.15}$/Si material in both inert and oxidizing ambients over the same temperature range has allowed estimation of the enhancement factor of interdiffusion under interstitial injection and equilibrium defect concentration conditions. Consequently, an estimate of the fractional contribution of interstitial and vacancy point defects to interdiffusion in $Si_{0.85}Ge_{0.15}$/Si SQWs has been made. Due to the nonpseudomorphic nature of the SiGe/Si structure used in this investigation, misfit and threading dislocations are expected in the as-grown samples. Because of the presence of strain and dislocations in the $Si_{0.85}Ge_{0.15}$ layer, our results are currently limited to the specific composition and layer structure investigated. Transmission electron microscopy (TEM) has been used to monitor the extent of dislocation generation and propagation upon annealing. In-

[a]Electronic mail: mgrig@tec.ufl.edu

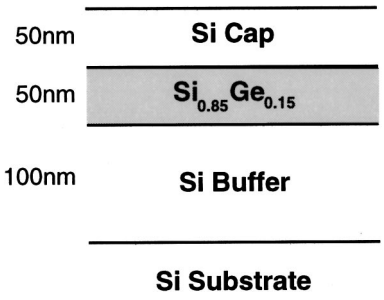

FIG. 1. Schematic representation of the $Si/Si_{1-x}Ge_x$ test structure.

vestigation of a $Si/Si_{1-x}Ge_x/Si$ structure with a buried boron (B) marker layer in the Si buffer region has addressed the impact of dislocated $Si_{1-x}Ge_x$ layers on nonequilibrium interstitial concentrations and any resulting variations in interdiffusion behavior.

EXPERIMENT

A SQW test structure, shown in Fig. 1, was grown using an ASM Epsilon 1 vapor phase epitaxy reactor. The structure consisted of a lightly *p*-doped (100) Si substrate with an undoped 100 nm Si buffer, followed by an undoped 50 nm $Si_{0.85}Ge_{0.15}$ layer and an undoped 50 nm Si cap. The $Si_{0.85}Ge_{0.15}$ layer was grown at a temperature of 700 °C at a rate of 18.8 nm/min, using $SiCl_2H_2$ (dichlorosilane), GeH_4 (germane), and hydrogen (H_2) as the carrier gas. The silicon layers were grown at a temperature of 700 °C at a rate of 5.0 nm/min using dichlorosilane and H_2 as the carrier gas. The Ge concentration of the $Si_{1-x}Ge_x$ layer was verified by Rutherford backscattering spectroscopy (RBS) using He^{2+} ions with a beam current of 10 nA and a collector charge of 4 mC. Each sample was rotated 10° and tilted 10° to prevent channeling. Layer thicknesses were verified by cross-sectional TEM using a JEOL 200CX instrument.

The Ge depth versus concentration profiles for as-grown and annealed samples were determined by SIMS using a Perkin Elmer PHI 6600 quadrapole analyzer with 6 keV O_2^+ ions, at a typical sputter rate of 24 nm/min, and a 60° incident angle. The profile depth scales were determined from Tencor Alpha-Step 500 surface profiler measurements of the SIMS sputtered craters. The variation of the sputter rate in the SIMS analysis was accounted for by a linearization technique which relates the secondary ion signal of the Ge to the secondary ion signal of the Si based on the counts from a sample of known Ge concentration using RBS.[8,9] The depth scale of the SIMS profiles of the annealed samples were laterally shifted no more than 20 nm (within one standard deviation, estimated at 0.05, in relative depth scale error of SIMS)[5] so that the peaks aligned with that of the as-grown profile. The Ge concentration scale of the SIMS profiles was standardized by equalizing the total dosage in each peak.

Samples annealed at high temperature and short time (less than approximately 5 min) in Ar (inert ambient) and O_2 (oxidizing ambient) were processed in an AG Associates Heatpulse 2101 rapid thermal processor (RTP). The Heatpulse 2101 controls the temperature of the wafer through the use of an IRCON optical pyrometer and closed loop feedback software. The RTP temperature for these investigations was initially calibrated through oxide thickness measurements.[10,11] To more accurately determine the RTP calibration, a thermocouple wafer was also used to calibrate the pyrometer.[12] Before annealing, the test wafer was cut into 1×1 cm pieces which were cleaned using a regimen of de-ionized water, H_2SO_4:H_2O_2 (1:2) and H_2O:HF (10:1), and then dried with N_2. Samples were rapid thermal processed with ambient gases (Ar, O_2) flowing at 1.5 slm.

Samples annealed for longer than 5 min in either N_2 (inert ambient) or O_2 (oxidizing ambient) were processed in a Thermco furnace. The $Si/Si_{1-x}Ge_x$ test pieces underwent preparations identical to those for RTP. Since Ar and N_2 have similar thermal conductivities, the thermal profiles of samples processed in these gases are expected to be similar. Therefore, the diffusion profiles of the samples processed in inert ambient by RTP and furnace are considered comparable in this investigation.

EXTRACTION OF DIFFUSION COEFFICIENTS

The approach used in all simulations in this investigation was to model the $Si_{1-x}Ge_x$ alloy regions as Ge dopant in the Si lattice. This allows one equation describing mobile and immobile Ge to be written, in which the expression of interest is the ratio of the two. This ratio of mobile to immobile Ge concentrations was calculated by assuming local equilibrium between the two species. Ultimately, the simulation used expressions for interstitial and vacancy concentrations as well as total Ge concentration to solve the diffusion equations and provide a final depth versus concentration profile.[13]

The as-grown Ge profile determined from SIMS was used as the initial profile for the Ge diffusion simulations. The simulated Ge depth versus concentration profile after processing was generated using Fick's second law with the diffusivity described by an Arrhenius expression. The effective Ge diffusivity for each processing time and temperature, in both ambients, was extracted by fitting the profile calculated by simulations to the standardized experimental SIMS profile according to the procedure outlined in Gossmann *et al.*[5] The value of the diffusivity was considered a function of temperature only, ignoring possible concentration and stress dependencies. Diffusion was simulated for one dimension only, in the direction perpendicular to the sample surface. Electric field effects were ignored due to two simplifying assumptions: (1) Fermi level effects of ionized defects were assumed to be orders of magnitude smaller than dopant concentrations, and therefore too small to contribute to an electric field and (2) the substitutional dopant atom (Ge) is neutral within the host lattice (Si).

The standard approach previously described by Fahey *et al.*[6] was used to estimate the fractional interstitial and vacancy components, f_I and f_V. The extracted effective diffusivities in inert ambient, D^*, can be defined as the sum of the effective interstitial and vacancy diffusivities in inert ambient, D_I^* and D_V^*

$$D^* = D_I^* + D_V^*, \tag{1}$$

TABLE I. Extracted diffusivity values for the test structure in inert and oxidizing ambients.

T (°C)	Time (min)	D_{Ge}^{Inert}(cm^2/s)	D_{Ge}^{Ox}(cm^2/s)
900	330	1.70×10^{-17}	2.32×10^{-17}
	980	2.29×10^{-17}	1.27×10^{-17}
	1532	2.08×10^{-17}	6.34×10^{-18}
	2206	2.08×10^{-17}	...
1000	43	3.00×10^{-16}	3.28×10^{-16}
	55	3.29×10^{-16}	4.56×10^{-16}
	87	3.29×10^{-16}	3.94×10^{-16}
	125	3.00×10^{-16}	2.74×10^{-16}
1100	1	5.20×10^{-14}	1.14×10^{-14}
	2	7.93×10^{-14}	5.20×10^{-14}
	3	6.69×10^{-14}	4.21×10^{-14}
	4	8.60×10^{-14}	7.93×10^{-14}
1200	1	2.38×10^{-12}	4.05×10^{-13}
	1.5	6.00×10^{-13}	4.93×10^{-13}
	2	1.08×10^{-12}	4.56×10^{-13}
	3	1.08×10^{-12}	4.56×10^{-13}

which allows the fraction of diffusion occurring via interstitials to be defined as

$$f_I=\frac{D_I^*}{D_I^*+D_V^*} \quad \text{with} \quad f_V=1-f_I. \tag{2}$$

To estimate the fractional interstitial and vacancy components, f_I and f_V, for each processing temperature from oxidizing ambient experiments, the D^* extracted from inert ambient experiments was proportioned into interstitial and vacancy contributions according to Eq. (1), resulting in a f_I as defined by Eq. (2). These values of D^*, f_I, and f_V were used to calculate a diffusivity under nonequilibrium point defect conditions

$$\frac{D}{D^*}=f_I\frac{C_I}{C_I^*}+f_V\frac{C_V}{C_V^*}, \tag{3}$$

where C_I and C_V are the actual concentrations of interstitials and vacancies, and C_I^* and C_V^* are the equilibrium concentrations of interstitials and vacancies. The values of C_I/C_I^* and C_V/C_V^* used for each temperature under interstitial injection due to dry oxidization were those reported by Packan[15] for enhanced diffusion of phosphorous in silicon, assuming an f_I of $\approx$1. The error in the determined diffusion coefficients was estimated using a Monte Carlo approach detailed in Gossmann *et al.*,[5] in which a mean D and its standard deviation are calculated from numerically generated pairs of concentration and depth values based on the original experimental data sets. The results are given as the error bars in the figures.

RESULTS

The extracted diffusivity values after processing inert and oxidizing ambients are given in Table I. It was determined after error analysis, that in both inert and oxidizing ambients, the diffusivities are constant (within error of each other) with increasing time for all temperatures investigated. The value of the diffusivity in an oxidizing ambient for an anneal temperature 900 °C and time 2206 min could not be extracted because the 50 nm Si cap had been consumed by the oxide and oxidation of the $Si_{1-x}Ge_x$ layer had occurred. The values of the diffusivities as a function of reciprocal temperature in inert and oxidizing ambients are shown in Fig. 2. Fitting this data to Arrhenius expressions results in the following equations when the interdiffusion is carried out in inert and oxidizing ambients:

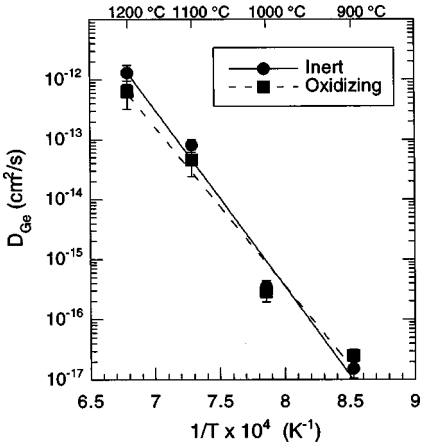

FIG. 2. Effective Ge diffusivity of the test structure as a function of processing temperature in inert and oxidizing ambients.

$$D_{Ge}^{Inert}=1.6\times10^8\exp(-5.87\,\text{eV}\pm0.14/\text{kT})\ \text{cm}^2/\text{s}, \tag{4}$$

$$D_{Ge}^{Ox}=6.1\times10^5\exp(-5.27\,\text{eV}\pm0.11/\text{kT})\ \text{cm}^2/\text{s}. \tag{5}$$

Thus an activation energy for interdiffusion of $Si_{1-x}Ge_x$/Si layers under interstitial injection has been directly determined from experiment.

The thickness of the $Si_{0.85}Ge_{0.15}$ layer in the SQW test structure, 50 nm, was greater than the critical thickness ($\sim$30 nm) of a capped $Si_{1-x}Ge_x$ layer with a Ge composition of 0.15.[14] Plan view TEM (PTEM) analysis at a magnification of $\times$20k showed the as-grown structure exhibited strain relief through an array of misfit dislocations spaced an average of approximately 1 μm apart, signifying that the structure is partially relaxed through the presence of dislocations prior to any high-temperature processing [Fig. 3(a)]. The initial stage of high-temperature treatment of these structures could cause additional strain relaxation by formation and propagation of misfit and threading dislocations as well as strain-enhanced diffusion, thereby affecting the diffusivity. PTEM performed at a magnification of $\times$20k of the SQW structure after annealing at 900 °C for 330 min confirms a significant increase in the misfit dislocation density, as well as an origination of curved segments which are most likely expanded threading dislocations seen from an overhead perspective [Fig. 3(b)]. All plan views were taken near the [100] zone axis so that the sample was perpendicular to the electron beam and $\mathbf{g}_{220}$ weak beam dark field imaging conditions were used.

In addition to strain release, these dislocations (in either the Si or $Si_{1-x}Ge_x$ layer) can possibly trap interstitials injected during the oxidation process, thus severely limiting the role these excess point defects play in Ge diffusion in the $Si_{1-x}Ge_x$ layer. Thus, it was necessary to determine whether

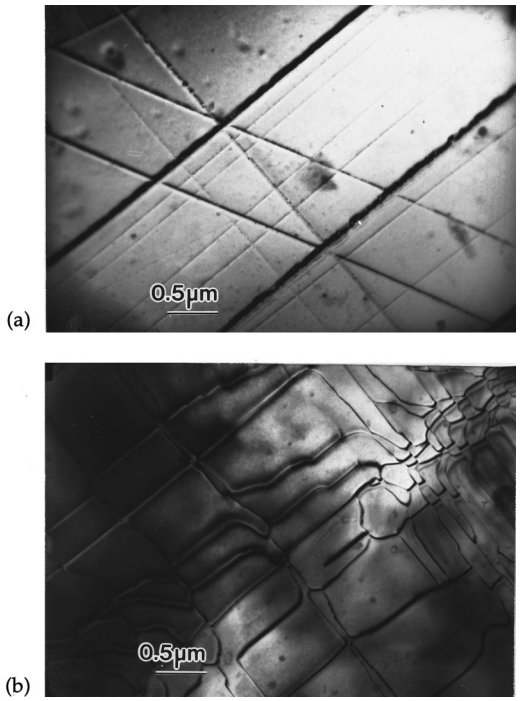

FIG. 3. Plan view TEM images of test structure (a) as-grown and (b) after anneal at 900 °C for 330 min.

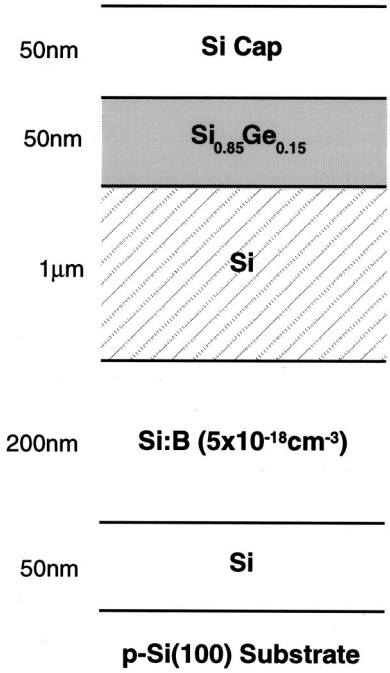

FIG. 4. Schematic representation of the test structure SQW/B. A buried boron marker layer is positioned below $Si/Si_{1-x}Ge_x/Si$ layers similar to the SQW test structure.

the injected interstitials were indeed trapped by the dislocations or whether they traveled to and throughout the $Si_{1-x}Ge_x$ layer to participate in the diffusion process.

A test structure, hereafter referred to as SQW/B, was grown which consisted of a lightly doped *p*-type Si (100) substrate with a 50 nm Si buffer, followed by a 200 nm boron-doped Si layer, with a B concentration of $5\times10^{18}\,cm^{-3}$. A layer structure identical to that of the original SQW test structure was grown on top of these layers: a $1\mu m$ Si ''buffer'' layer, followed by a 50 nm undoped $Si_{0.85}Ge_{0.15}$ layer and an undoped 50 nm Si cap layer (Fig. 4).

It is widely established that boron diffuses in Si predominantly through an interstitial mechanism.[6] If the B in the marker layer underneath the $Si_{1-x}Ge_x$ layer shows enhanced diffusion after annealing in an interstitial-injecting (O_2) ambient as compared to an inert (N_2/Ar) ambient, it can be concluded that the interstitials are indeed traveling throughout the $Si_{1-x}Ge_x$ layer without significant capture by dislocations. The interstitials would therefore be available to facilitate the diffusion process and any differences in Ge diffusion seen between the inert and oxidizing ambients could be attributed to the injection of excess interstitials.

The SQW/B structure was furnace annealed at 900 °C for 330 min and at 1000 °C for 43 min in both N_2 and O_2. The SQW/B structure was also rapid thermally processed at 1100 °C for 2 min and at 1200 °C for 1 min in Ar and O_2. These selected anneal conditions are identical to four anneal conditions used for the SQW test structure. The B profiles before and after anneal were determined using SIMS (Fig. 5). Qualitatively, B diffusion was greater in O_2 ambient than in Ar/N_2 ambient for all processing temperatures.

FLOOPS was used to determine the quantitative transport of interstitials through the $Si_{1-x}Ge_x$ layer to the B marker layer. The SIMS profile of the as-grown boron marker layer was used as the initial B profile. The diffusivity of B in Si under both oxidizing[15] and inert[16] conditions is well established, so the diffusion coefficient was maintained constant while the *time* of anneal was changed in the simulations until the calculated profile fit the experimental SIMS profile after anneal. Table II gives a summary of the anneal times calculated by simulation compared to the actual anneal times in inert and oxidizing ambients. The ratio of these times was used calculate the actual C_I/C_I^* values in inert and oxidizing ambients compared to the default values used in simulations. A corresponding C_V/C_V^* range in inert ambient was estimated by designating either an upper limit in which vacancies remain at their equilibrium concentration, such that $C_V/C_V^*=1$, or a lower limit in which C_IC_V

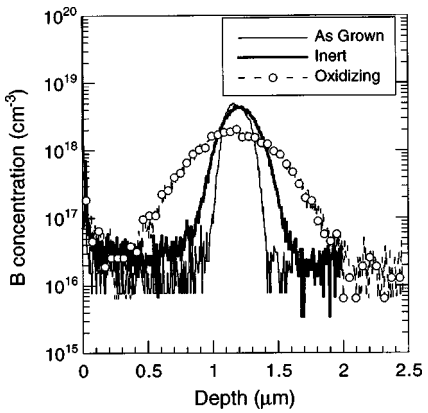

FIG. 5. Diffusion of the as-grown B marker layer in both ambients. The sample was annealed at 1100 °C for 2 min. Diffusion of B in oxidizing ambient is noticeably greater than in inert ambient.

TABLE II. Anneal times needed in simulations to achieve actual B diffusion profiles.

T (°C)	Actual anneal time (min)	t_{Ar} (min)	t_{Ox} (min)
900	330	1100	2200
1000	43	90	160
1100	2	6	32
1200	1	0.7	0.6

$=C_I^* C_V^*$. A constant f_I was assumed for a constant temperature regardless of the processing ambient. Equation 3 was then solved simultaneously for D^* and f_I in both inert and oxidizing ambients for both the upper and lower limit cases for the specific processing temperatures and times used for the B marker layer experiments. Values of D^*, C_I/C_I^*, C_V/C_V^*, and f_I for inert and oxidizing experiments for the processing temperatures and times investigated in the B marker layer experiments are given in Table III. The first row for each processing time represents the results using the lower bound for C_V/C_V^*, while the second row represents the results using the upper bound. The cells with no data represent conditions in which the particular bound did not provide reasonable results for either f_I or C_I/C_I^*.

It is important to note here that these D^* and f_I values apply most rigorously to only the processing temperatures and times at which they were extracted from the B marker layer experiments. The analysis was adapted and extended to address the additional processing times in Table I by assuming D^* and f_I values remained constant with increasing processing time at a constant temperature, while the C_I/C_I^* and C_V/C_V^* values were allowed to change with time. It has been widely accepted that nonequilibrium concentrations of interstitials and vacancies vary with processing time.[6] Values of D^*, C_I/C_I^*, C_V/C_V^*, and f_I determined for inert and oxidizing experiments for the processing temperatures and times in Table I not investigated in the B marker layer experiments are given in Griglione.[17]

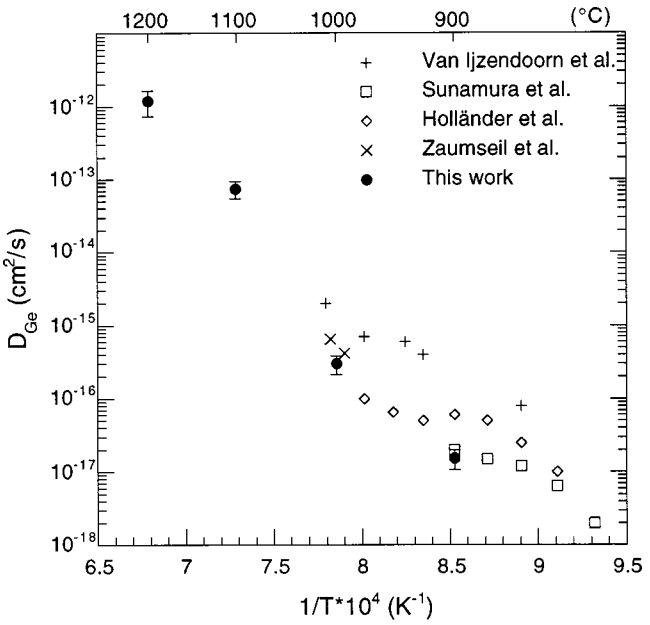

FIG. 6. Diffusivities of Ge in $Si/Si_{1-x}Ge_x/Si$ SQWs from previous studies and this work.

DISCUSSION

Previously reported values for the diffusivity of Ge in $Si/Si_{1-x}Ge_x/Si$ structures in inert ambient are shown in Fig. 6.[18–21] Sunamura *et al.*[18] investigated interdiffusion of a SQW structure with a 7.3 nm (below critical thickness) $Si_{0.84}Ge_{0.16}$ layer, annealed from 800 to 900 °C. Van Ijzendoorn *et al.*[21] studied a SQW very similar to that of this

TABLE III. Fractional interstitial components and modified diffusivities and point defect supersaturations determined for diffusion in (a) inert and (b) oxidizing ambients.

	T (°C)	Time (min)	D (cm^2/s)	D^* (cm^2/s)	C_I/C_I^*	C_V/C_V^*	f_I
(a)							
	900	330	1.70×10^{-17}	1.28×10^{-17}	3.33	1.00	0.140
			1.70×10^{-17}	2.38×10^{-17}	3.33	0.330	0.127
	1000	43	3.00×10^{-16}	2.82×10^{-16}	2.09	1.00	0.059
			3.00×10^{-16}	4.19×10^{-16}	2.09	0.480	0.148
	1100	1	5.20×10^{-14}	7.77×10^{-14}	⋯	1.00	0.010
			5.20×10^{-14}	2.19×10^{-13}	5.69	0.176	0.011
	1200	1	2.38×10^{-12}	⋯	0.700	1.00	⋯
			2.38×10^{-12}	1.70×10^{-12}	0.700	1.43	0.045
(b)							
	900	330	2.32×10^{-17}	1.28×10^{-17}	6.67	1.00	0.140
			2.32×10^{-17}	2.38×10^{-17}	6.67	0.150	0.127
	1000	43	3.28×10^{-16}	2.82×10^{-16}	3.72	1.00	0.059
			3.28×10^{-16}	4.19×10^{-16}	3.72	0.480	0.148
	1100	1	1.14×10^{-14}	7.77×10^{-14}	⋯	0.501	0.010
			1.14×10^{-14}	2.19×10^{-13}	28.9	0.035	0.011
	1200	1	4.05×10^{-13}	⋯	0.600	1.00	⋯
			4.05×10^{-13}	1.70×10^{-12}	0.600	1.67	0.045

investigation, containing a 50 nm $Si_{0.83}Ge_{0.17}$ layer, annealed from 850 to 1010 °C. Holländer *et al.*[19] examined a SQW with a $Si_{0.80}Ge_{0.20}$ layer, 10 nm thick (below critical thickness), thermally processed from 825 to 975 °C. Zaumseil *et al.*[20] investigated a highly strained SQW containing a 62-nm-thick $Si_{0.751}Ge_{0.249}$ layer annealed at 993 and 1006 °C. The diffusivities determined from this study at 900 and 1000 °C are slightly lower but still agree well with the diffusivities reported in the literature over the temperature range 800–1010 °C. The values at 1100 and 1200 °C from this study are the only known diffusivities reported for this temperature range. This work reports diffusivities that span over five orders of magnitude (10^{-17}–10^{-12} cm^2/s) while previous studies report diffusivities that extend over only two orders of magnitude at most.

The activation energy of Ge diffusion in $Si/Si_{1-x}Ge_x/Si$ in inert ambient determined in this study, $5.87\,eV \pm 0.14$, is substantially higher than activation energies previously reported.[18,21] Van Ijzendoorn *et al.* and Sunamura *et al.* both reported activation energies of approximately 2.5 eV for SQWs with Ge compositions $x=0.17$ and 0.16, respectively. While the thickness of the SQW studied in Sunamura *et al.* was below critical thickness, the thickness of the SQW studied by Van Ijzendoorn *et al.* was above critical thickness and the same as that of this study (50 nm). The larger activation energy determined from this study could possibly be attributed to the difference in temperature range investigated. The studies of Van Ijzendoorn *et al.* and Sunamura *et al.* were conducted in a lower, narrower temperature range from 800 to 1010 °C. An activation energy of 4.06 eV would be calculated for this study if only this lower, narrower temperature range was examined. While still higher than the ~2.5 eV of Van Ijzendoorn *et al.* and Sunamura *et al.*, the difference is certainly more comparable. Another reason for the discrepancy could be due to the difference in the method of extracting the diffusion coefficient. Van Ijzendoorn *et al.* calculated the diffusion coefficient using full width at half maximum analysis of either the tail or peak of RBS spectra. Calculations from the two sections of the profile resulted in diffusion coefficients which differed remarkably by 1–2 orders of magnitude. Sunamura *et al.* extracted the diffusion coefficients using the energy blue shifts of photoluminescence and a one-dimensional diffusion equation in the form of a difference equation. Finally, it should be noted that the activation energy calculated in this work (~5.8 eV) physically compares with the reported value for the Ge tracer diffusivity in pure Si.[6] There is a possibility that after the structure has relaxed during the very first stage of processing, Ge diffusion in relaxed $Si_{1-x}Ge_x$ is similar to Ge diffusion in bulk (relaxed) Si.

At all temperatures, the diffusion profiles in an oxidizing ambient are very similar to the diffusion profiles in an inert ambient (Fig. 7). Diffusivities extracted are the same, within error, for temperatures 900 and 1000 °C, as illustrated in Fig. 2. This indicates that a supersaturation of interstitials has very little effect on Ge diffusion at these temperatures and that vacancies are the dominant diffusing species. Diffusivities extracted for anneals at 1100 and 1200 °C are also within error of each other, as illustrated in Fig. 2. The difference in

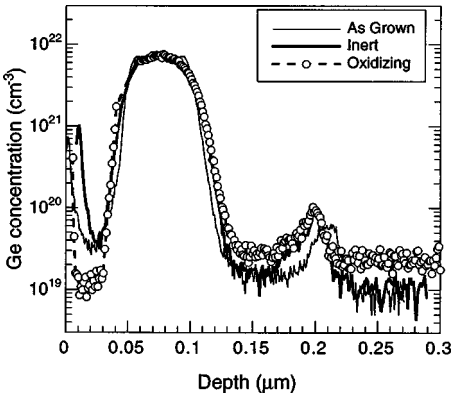

FIG. 7. Comparison of Ge SIMS profiles in inert and oxidizing ambients after processing at 900 °C for 330 min.

diffusion coefficients increases moderately with increasing temperature, with the maximum divergence occurring at 1200 °C. At these higher temperatures, diffusivities are moderately *smaller* in oxidizing ambient than inert, therefore diffusion is temperately retarded under interstitial supersaturation. This leads to the conclusion that interstitials play a minimal role in diffusion at all temperatures and at high temperature, injected interstitials may even combine with vacancies, reducing the vacancy concentration, and retarding vacancy-dependent diffusion.

The activation energy of $5.27\,eV \pm 0.11$ calculated for interdiffusion in oxidizing ambient is the activation energy for $Si_{1-x}Ge_x/Si$ interdiffusion under interstitial injection. This activation energy is similar to that in inert ambient and reinforces the conclusion that interstitials do not have a significant role in the interdiffusion process.

The boron marker layer experiment described previously was employed to determine whether excess interstitials injected through surface oxidation are captured by dislocations or travel through the dislocated layers unimpeded. Qualitatively, at all anneal temperatures the boron marker layer diffused farther in oxidizing ambient than in inert ambient (Fig. 5). This result indicates that interstitials are transported through the dislocated Si and $Si_{1-x}Ge_x$ layers and reach the buried B layer to enhance its diffusion. It can therefore be concluded that interstitials injected through the surface oxidation process are available to aid in the Ge diffusion across Si and $Si_{1-x}Ge_x$ layers. Quantitatively, this conclusion requires further investigation. The processing times listed in Table II result in simulated enhancements which are greater than actual enhancements for each anneal temperature. The enhancements predicted by simulations vary from 1.78 to 5.33. This result, along with the fact that enhancement of B diffusion is indeed seen in the SIMS profiles, allows the expression

$$1 < \text{enh (actual)} < \text{enh (FLOOPS)} \tag{6}$$

to be written. Interstitials are captured but not completely.

Fang[22] also used the presence of misfit dislocations nucleated by an unstably strained $Si_{1-x}Ge_x$ layer to determine whether the dislocations act as an interstitial barrier. Boron marker layers were grown in and on either side of a $Si_{0.80}Ge_{0.20}$ layer of varying thickness and the resulting

samples were annealed at 850 °C in either an inert or dry O_2 ambient, much like the experiment performed earlier. Fang concluded that under interstitial supersaturation, dislocations act as interstitial sinks, while under inert ambient they do not. Kuo *et al.*[23] also examined the effects of oxidation upon diffusion of boron marker layers in $Si/Si_{1-x}Ge_x/Si$ structures similar to those used in Fang. Unlike the results of Fang, they found that a thin $Si_{1-x}Ge_x$ layer does not interfere with the motion of interstitials. The results of this investigation support the conclusion that a portion of interstitials injected during surface oxidation travel throughout the $Si_{1-x}Ge_x$ layer and beyond, while the remaining excess interstitials are captured by dislocations. This merely means that the f_I estimated in this work is a lower bound for the fraction of Ge diffusion occurring via interstitials and that dislocations likely alter C_I/C_I^* and C_V/C_V^* ratios.

The calculated C_I/C_I^* values given in Table III were indeed different, and in most cases lower, than previously reported values[14,24] for intrinsic and interstitial supersaturation conditions. Both intrinsic and injected interstitials were captured by the dislocations, altering both C_I/C_I^* and C_V/C_V^*. A general result of the B marker layer analysis was that the lower bound for C_V/C_V^* seemed to result in C_I/C_I^* values that were physically more reasonable than those resulting from the higher bound. This is most apparent at 1200 °C where the limit of $C_V/C_V^*=1$ could provide no reasonable results. These results indicate that the point defect balance is governed by the relation $C_IC_V=C_I^*C_V^*$.

Using this conclusion and the values from Table III, f_I values for diffusion in the SQW were estimated. The lower bound of C_V/C_V^* and the corresponding C_I/C_I^* values resulted in similar f_I values of 0.127 and 0.148 for 900 and 1000 °C, respectively. The values dropped significantly at 1100 and 1200 °C to approximately 0.01 and 0.03, respectively. It would seem that there is a significant change in the respective contributions of interstitial and vacancy point defects between 1000 and 1100 °C. The only other estimate of f_I determined from oxidation studies was made by Cowern *et al.*,[25] who reported an f_I value of 0.220 at 875 °C. While the value of Cowern *et al.* is greater than values estimated at 900 °C from this work, it is reasonably similar and corroborates a diffusion mechanism dominated by vacancies.

SUMMARY

The diffusion model used in simulations, while employing several simplifying assumptions, proved to be a satisfactory first effort at predicting Ge diffusion behavior. Diffusivities extracted in an inert ambient at low temperature agreed well with previously reported values. A major contribution of this work was to extend the anneal temperature regime beyond 1000 °C providing diffusivity values for temperatures up to 1200 °C. An activation energy of diffusion of $5.87\,\text{eV}\pm0.14$ was extracted, which is much higher than previously reported values. This investigation, however, covered a larger temperature range and provided diffusivities spanning five orders of magnitude, therefore, the extracted activation energy could be considered more comprehensive than any previously reported.

Diffusivities extracted under interstitial injection conditions were reported with a resulting activation energy for diffusion of $5.27\,\text{eV}\pm0.11$. No significant enhancement or retardation of Ge diffusion was seen in oxidizing ambient when compared to inert ambient. Lower limits of f_I of approximately 0.10 at the lower temperatures and 0.02 at the higher temperatures were estimated from oxidizing experiments. Diffusion seems to be dominated by vacancies at all processing temperatures. Finally, a portion of injected excess interstitials proved to be captured by misfit dislocations, however, enhancement of boron marker layer diffusion under oxidizing ambient compared to inert ambient established that a modest amount of excess interstitials are available to participate in the diffusion process.

ACKNOWLEDGMENTS

The authors would like to thank Dr. Margarida Puga-Lambers of Microfabritech for SIMS measurements, Dr. Wish Krishnamoorthy of University of Florida for TEM analysis, and Dr. Doug Meyer of ASM Epitaxy for assistance with growth of the structures.

[1] U. König, IEEE Colloquium Advances in Semiconductor Devices 1999/025 (1999), p. 48.
[2] S. Subbana, D. Ahigren, D. Harame, and B. Meyerson, *1999 IEEE Int. Solid-State Circuits Conf. Digest of Tech. Papers* (IEEE, Piscataway, NJ, 1999), p. 508.
[3] G. Freeman *et al.*, Mater. Res. Soc. Symp. Proc. **533**, 19 (1998).
[4] M. E. Law, *FLOOPS User's Manual* (University of Florida, Gainesville, FL, 1996).
[5] H.-J. Gossmann, A. M. Vredenberg, C. S. Rafferty, H. S. Luftman, F. C. Unterwald, D. C. Jacobson, T. Boone, and J. M. Poate, J. Appl. Phys. **74**, 3150 (1993).
[6] P. M. Fahey, P. B. Griffin, and J. D. Plummer, Rev. Mod. Phys. **61**, 289 (1989).
[7] S. M. Hu, J. Electrochem. Soc. **139**, 2066 (1992).
[8] G. Prudon, B. Gautier, S. Berthelemy, J. C. Dupuy, C. Dubois, J. Schmitt, J. Delmas, and J. P. Vallard, Proc. of the 11th Inter. Conf. on Secondary Ion Mass Spectrometry (SIMS XI) (1997), Vol. 11, p. 339.
[9] J. P. Newey, D. J. Robbins, and D. Wallis, Proc. of the 11th Inter. Conf. on Secondary Ion Mass Spectrometry (SIMS XI) (1997), Vol. 11, p. 979.
[10] M. M. Moslehi, S. C. Shatas, and K. C. Saraswat, Appl. Phys. Lett. **47**, 1353 (1985).
[11] N. Gonon, A. Gagnaire, D. Barbier, and A. Glachant, J. Appl. Phys. **76**, 5242 (1994).
[12] J. L. Hoyt, K. E. Williams, and J. F. Gibbons, US Patent No. 4,787,551 (1998).
[13] D. Mathiot and J. C. Pfister, J. Appl. Phys. **55**, 3518 (1984).
[14] S. C. Jain, *Germanium-Silicon Strained Layers and Heterostructures* (Academic, New York, 1994).
[15] P. A. Packan and J. D. Plummer, J. Appl. Phys. **68**, 4327 (1990).
[16] D. Barbuscia, Int. Electron. Dev. Meet. **84**, 757 (1984).
[17] M. Griglione, Ph.D. thesis, University of Florida, April 1999.
[18] H. Sunamura, S. Fukatsu, N. Usami, and Y. Shiraki, Jpn. J. Appl. Phys., Part 1 **33**, 2344 (1994).
[19] B. Holländer, S. Mantl, B. Stritzker, H. Jorke, and E. Kasper, J. Mater. Res. **4**, 163 (1989).
[20] P. Zaumseil, U. Jagdhold, and D. Krüger, J. Appl. Phys. **76**, 2191 (1994).
[21] L. J. Van Ijzendoorn, G. F. A. Van De Walle, A. A. Van Gorkum, A. M. L. Theunissen, R. A. Van de Heuvel, and J. H. Barrett, Nucl. Instrum. Methods Phys. Res. B **50**, 127 (1990).
[22] W. T. C. Fang, Ph.D. thesis, Stanford University, 1996.
[23] P. Kuo, J. L. Hoyt, J. F. Gibbons, J. E. Turner, and D. Lefforge, Appl. Phys. Lett. **67**, 706 (1995).
[24] P. Packan, Ph.D. thesis, Stanford University, 1991.
[25] N. E. B. Cowern, W. J. Kersten, R. C. M. de Kruif, J. G. M. van Berkum, W. B. de Boer, D. J. Gravesteijn, and C. W. T. Bulle-Liewma, Proceedings of the Electrochem. Soc. (1996), Vol. 964, p. 195.